NASA Technical Memorandum 104773

IN-34

174955

P.20

Space Shuttle Orbiter Thermal Protection System Design and Flight Experience

Donald M. Curry

July 1993

NASA Technical Memorandum 104773

Space Shuttle Orbiter Thermal Protection System Design and Flight Experience

Donald M. Curry
Lyndon B. Johnson Space Center
Houston, Texas

Presented at the
First ESA/ESTEC Workshop on Thermal Protection Systems
Noordwijk, the Netherlands, May 5-7, 1993

National Aeronautics and
Space Administration

CONTENTS

Section	Page
ABSTRACT	1
INTRODUCTION	1
THERMAL PROTECTION SYSTEM DESIGN	1
Aerothermodynamic Environment	1
TPS Materials/Distribution	3
FLIGHT EXPERIENCE	6
Aerothermodynamic Environment	6
TPS Thermal Performance	7
TPS Thermal Mechanical Performance	8
Concluding Remarks	14
BIBLIOGRAPHY	14

TABLES

Table		Page
1	ORBITER THERMAL PROTECTION SYSTEM (TPS) MATERIAL TEMPERATURE LIMITS	3
2	REINFORCED CARBON-CARBON DESIGN ALLOWABLES	4
3	RSI TYPICAL PROPERTIES	4

FIGURES

Figure		Page
1	DESIGN ORBITER SURFACE TEMPERATURES, °C [ASCENT AND REENTRY TRAJECTORIES]	2
2	THERMAL PROTECTION SYSTEM, ORBITER 103 AND SUBSEQUENT ORBITERS	2
3	RSI SYSTEM CONFIGURATION	5
4	WING LEADING EDGE SYSTEM COMPONENTS	5
5	NOSE CAP SYSTEM COMPONENTS	5
6	RCC CHIN PANEL SYSTEM COMPONENTS	6
7	ORBITER INFERRED AND PREDICTED HEAT FLUX, STS-3	6
8	ORBITER ENTRY TEMPERATURES	6
9	STS-2, STS-3, AND STS-5 PEAK IML TEMPERATURE (°C) LESS WING LEADING EDGE	7
10	WING LEADING EDGE SPANWISE HEATING RATE	7
11	PANEL 9 PEAK TEMPERATURES, °C [X/X/X/X/X = STS-1/STS-2/STS-3/STS-4/STS-5, ORBITER VEHICLE 102]	7
12	WING LEADING EDGE - PANEL 9 RCC SURFACE TEMPERATURES FOR HEAVYWEIGHT AND NOMINAL ENTRY	7
13	ACTIVE-PASSIVE TRANSITION OXYGEN PRESSURES COMPARISONS WITH FLIGHT CONDITIONS	8
14	ORBITER PEAK SURFACE TEMPERATURES	8
15	ORBITER MAXIMUM STRUCTURE TEMPERATURES	9
16	ORBITER DEBRIS DAMAGE SUMMARY FOR ENTIRE VEHICLE	9
17	DEBRIS DAMAGE LOCATIONS	9
18	RSI TILE IMPACT DAMAGE	10
19	WING DEBRIS IMPACT GOUGE	10
20	OV-104 WING LEADING EDGE, PANEL 10 RH OUTER MOLD LINE (OML)	11
21	OV-104 WING LEADING EDGE, PANEL 10 RH INNER MOLD LINE (IML)	11
22	ELEVON-ELEVON GAP HEATING/TILE SLUMPING	12
23	NOSE CAP LOWER SURFACE, INTERFACE DAMAGE, STS-5	12
24	NOSE LANDING GEAR DOOR THERMAL BARRIER	13
25	ORBITER WINDOW CONTAMINATION	13

SPACE SHUTTLE ORBITER THERMAL PROTECTION SYSTEM DESIGN AND FLIGHT EXPERIENCE

Donald M. Curry
NASA/Johnson Space Center
Houston, TX

ABSTRACT

The Space Shuttle Orbiter Thermal Protection System materials, design approaches associated with each material, and the operational performance experienced during fifty-five successful flights are described. The flights to date indicate that the thermal and structural design requirements have been met and that the overall performance has been outstanding.

INTRODUCTION

The Space Shuttle represents a revolution in manned, reusable space transportation systems. The development, fabrication, and fifty-five successful flights of a fully reusable, weight-efficient Orbiter thermal protection system (TPS) are major technical accomplishments in TPS materials and design approaches. The initial five Orbiter flights provided the detailed engineering data required to verify the TPS thermal performance, structural integrity, and reusability. Limited operational thermal data and postflight inspections are now providing the necessary data to ensure continued safety-of-flight performance.

The thermal protection for the Orbiter is designed to operate successfully over a spectrum of environments typical of both aircraft and spacecraft. During the ascent and entry phases of the mission, the Orbiter structure is maintained at temperatures less than 177°C (350°F). In addition to withstanding the thermal environments, the TPS must also perform satisfactorily for other induced environments, i.e., launch acoustics, structural deflections induced by aerodynamic loads, on-orbit cold soak, and natural environments, such as salt, fog, wind, and rain. The exterior surfaces of the TPS must provide an acceptable aerodynamic surface to avoid early tripping of the high-temperature boundary layer (from laminar to turbulent flow). This would significantly increase the thermal heat load to the structure. This requirement resulted in rigid fabrication tolerances during the manufacturing and installation phases of the TPS. The key driver to the design of the TPS has been the requirement for the TPS to function for 100 missions with minimal weight, maintenance, and refurbishment.

Selection and location of the various thermal protection materials applied to the Orbiter structure are based primarily on the inherent temperature capability of the materials. Two basic material systems used as the Orbiter TPS are reusable surface insulation (RSI) and reinforced carbon-carbon (RCC). The RSI can be further classified as rigid ceramic tiles and flexible blankets. The specific Orbiter locations for the RSI materials are based on predicted peak surface temperature and the material reuse temperature. The RCC is a unique structural material used in the regions of higher temperature (nose cap, wing leading edges, an area between the nose landing gear door and nose cap, and a small area surrounding the forward attach fitting of the external tank to the Orbiter).

This paper discusses the Orbiter's TPS design aspects, material characteristics, flight thermal performance, and operational experience. These data indicate that the TPS has met all design requirements, and the overall performance has been outstanding.

THERMAL PROTECTION SYSTEM DESIGN

Aerothermodynamic Environment

The TPS was designed for maximum reuse and minimum weight. Therefore, the entry aerothermodynamic environment played a major role in material selection, distribution, and the thickness required to limit the aluminum airframe to a peak temperature of 177°C (350°F). The methodology used in defining the Orbiter heating environment consisted of geometric flow models (i.e., flat plate, sphere, cone, wedge) and wind tunnel calibration of these heating models at flight conditions. A nominal trajectory for the most severe operational mission was selected to predict the design entry aerothermodynamic environment. Although the most severe operational mission was selected for the entry heating definition, a nominal trajectory with nominal heating, nominal material properties, and an aerodynamically smooth surface was used for the TPS design. Design heating environments were defined at approximately 2000 locations on the Orbiter to support material selection and sizing of the TPS. Figure 1 shows selected Orbiter peak design temperatures.

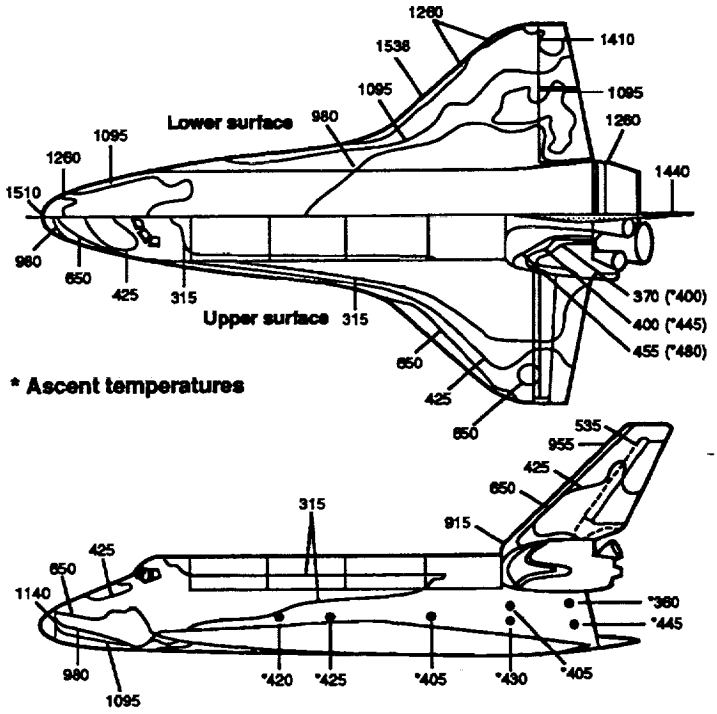

FIGURE 1: DESIGN ORBITER SURFACE TEMPERATURES, °C
[ASCENT AND REENTRY TRAJECTORIES]

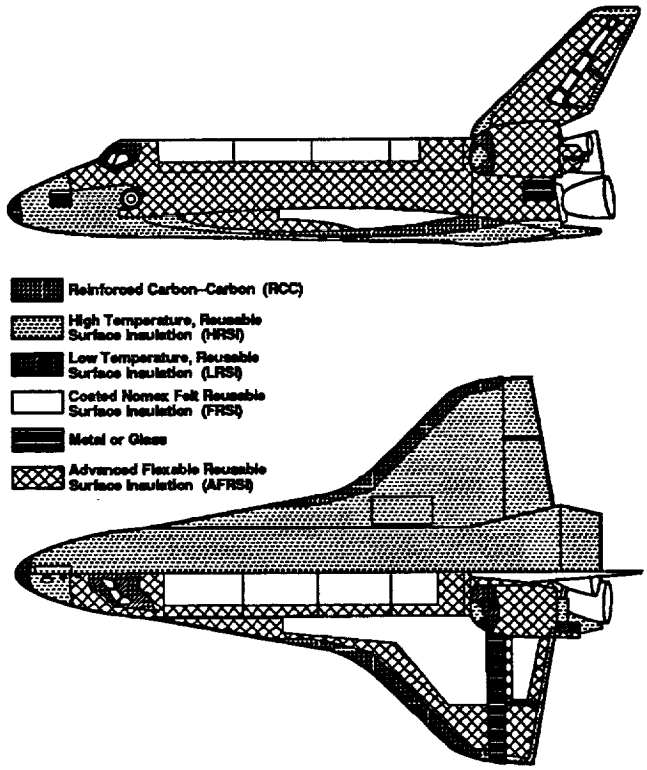

FIGURE 2: THERMAL PROTECTION SYSTEM, ORBITER 103 AND SUBSEQUENT ORBITERS

TPS Materials/Distribution

The Orbiter TPS consists of two basic material systems (figure 2): reinforced carbon-carbon (RCC) and reusable surface insulation (RSI). These materials were selected for high-temperature stability and weight efficiency, while protecting the Orbiter structure from the severe entry environment (Table 1). RCC is an all-carbon composite laminate fabricated in a multiple pyrolysis and densification process from a phenolic-graphite lay-up. An oxidation-resistant SiC coating is formed in a diffusion reaction process. Further oxidation resistance is provided by impregnation with tetraethyl-orthosilicate (TEOS) that when cured leaves a silicon dioxide residue throughout the coating and substrate. The final step in the fabrication process is the application of a surface sealant (sodium silicate/SiC mixture) to fill any remaining surface porosity or microcracks. The RCC is used where temperatures are predicted to exceed 1260°C (2300°F) for the RSI materials. Typical RCC design allowables are given in Table 2.

The RSI tiles are further classified as High Temperature Reusable Surface Insulation (HRSI) for areas where predicted temperatures range from 648°C (1200°F) to 1260°C (2300°F) and Low Temperature Reusable Surface Insulation (LRSI) for areas where the predicted temperature is between 371°C (700°F) to 648°C (1200°F). Fibrous refractory composite insulation (FRCI) is used in selected HRSI locations. Flexible Reusable Surface Insulation (FRSI) blankets are used for areas less than 371°C (700°F), and Advanced Flexible Reusable Surface Insulation (AFRSI) is used for areas less than 816°C (1500°F). The tiles are made of a low-density, high–purity silica 99.8-percent amorphous fiber insulation that is rigidized by ceramic bonding. The HRSI tiles have densities of 144 kg/m3 (9 lb/ft3) or 352 kg/m3 (22 lb/ft3) with a black Reaction Cured Glass (RCG) surface coating. The LRSI tiles (144 kg/m3) have a white RCG coating, which provides on-orbit thermal control. The FRCI tiles have a density of 192 kg/m3 (12 lb/ft3), and by adding an alumino-boro-silicate fiber to the silica tile slurry, they have improved strength, improved durability, and reduced sensitivity to RCG coating cracking. The FRSI is a Nomex felt coated with a white pigmented silicone elastomer to waterproof the felt and provide the required thermal and optical properties. The AFRSI is a low-density 176-kg/m3 (11 lb/ft3) fibrous, silica batting made up of high-purity silica, 99.8-percent amorphous silica fibers. This batting is sandwiched between an outer woven silica high-temperature fabric and an inner lower temperature woven glass fabric. The composite is sewn with silica thread, treated to provide water repellency, and coated with a ceramic coating to provide durability and resistance to damage. The FRCI and AFRSI were not part of the original TPS design, but were incorporated into the Orbiter fleet on the Challenger and subsequent Orbiters. The AFRSI blankets have been used to replace a vast majority of the original LRSI tiles, resulting in reduced fabrication, installation time and costs, and weight. The FRCI tiles are used in areas susceptible to handling/impact damage, adjacent to penetrations and thermal barriers, and aerosurface-trailing edges. Typical RSI properties are given in Table 3.

The RSI ceramic tiles are bonded to the Orbiter structure with a silicone adhesive and an intervening layer of nylon felt (figure 3).

TABLE 1: ORBITER THERMAL PROTECTION SYSTEM (TPS) MATERIAL TEMPERATURE LIMITS

Type of Insulation	Maximum operating temperature		Minimum operating temperature
	100-mission life	Single-mission life	
High temperature reusable surface insulation (HRSI)	1260 °C (2300 °F)[a] 1260 °C (2300 °F)[b]	1427 °C (2600 °F)[a] 1482 °C (2700 °F)[b]	-128 °C (-200 °F)
Low temperature reusable surface insulation (LRSI)	1093 °C (1200 °F)	1149 °C (2100 °F)	-128 °C (-200 °F)
Fibrous refractory composite insulation (FRCI)	1260 °C (2300 °F)	1427 °C (2600 °F)	-128 °C (-200 °F)
Felt reusable surface insulation (FRSI)	399 °C (750 °F)	482 °C (900 °F)	-128 °C (-200 °F)
Advanced flexible reusable surface insulation (AFRSI)	816 °C (1500 °F)	982 °C (1800 °F)	-128 °C (-200 °F)
Reinforced carbon-carbon (RCC)	1482 °C (2700 °F)	1816 °C (3300 °F)	[c]
Thermal window pane	956 °C (2600 °F)	–	[c]

NOTES:
a 144 kg/m^3 tile
b 352 kg/m^3 tile
c No lower limit identified

TABLE 2: REINFORCED CARBON-CARBON DESIGN ALLOWABLES

STRUCTURAL				
		Values as fabricated (not degraded for subsurface attack)		Design value with 0.15 kg/m^2 weight loss
Property	Ply	Room temperature	1371 °C	Room temperature
F_{Tu}, N/m^2	19	3.116×10^7	3.482×10^7	2.758×10^7
F_{cu}, N/m^2	19	10.411×10^7	10.687×10^7	9.618×10^7
F_{bu}, N/m^2	19	6.205×10^7	6.205×10^7	4.688×10^7
F_{su}, N/m^2	19	2.337×10^7	2.930×10^7	1.931×10^7
F_{ilt}, N/m^2	19	0.221×10^7	0.221×10^7	0.147×10^7
E_t, N/m^2	19	1.45×10^{10}	1.57×10^{10}	9.31×10^9
ρ kg/m^3	All	1656	1656	–

THERMAL			
	Values as fabricated (not degraded for subsurface attack)		
Property	Room temperature	816 °C	1371 °C
Emittance	0.78	0.89	0.81
Conductivity, || to laminate, W/m-k	6.49	11.83	11.83
Conductivity, ⊥ to laminate, W/m-k	4.32	7.64	7.64
Specific heat, J/Kg-K	795	1423	1674
Thermal expansion cm/cm-°C	1.35×10^{-6}	2.30×10^{-6}	2.83×10^{-6}

TABLE 3: RSI TYPICAL PROPERTIES

PROPERTY	RCG	LI-900	LI-2200	FRCI-12
Density, kg/m^3	2195	144	352	192
Tensile strength, N/m^2				
Thru-the-thickness	–	1.65×10^5	5.03×10^5	5.58×10^5
In-plane	2.76×10^7	4.62×10^5	12.4×10^5	17.72×10^5
Compressive strength, N/m^2				
Thru-the-thickness	–	1.93×10^5	8.96×10^5	9.10×10^5
In-plane	6.89×10^5	4.83×10^5	15.86×10^5	18.27×10^5
Thermal expansion, cm/cm-°C				
Thru-the-thickness	1.08×10^{-6}	7.20×10^{-7}	7.20×10^{-7}	1.26×10^{-6}
In-plane	1.08×10^{-6}	7.20×10^{-7}	7.20×10^{-7}	1.26×10^{-6}
Apparent thermal conductivity, W/m-K				
Thru-the-thickness				
21 °C @ 10^{-4} atm	1.44	0.014	0.032	0.019
538 °C @ 10^{-4} atm	–	0.045	0.059	0.049
In-plane				
21 °C @ 1 atm	1.44	0.083	0.105	0.076
538 °C @ 1 atm	–	0.156	0.180	0.163
Specific heat, J/kg-K	920	711	711	711
Dielectric constant	4.8	1.13	1.30	1.20
Loss tangent	.0030	.0004	.0016	.0009

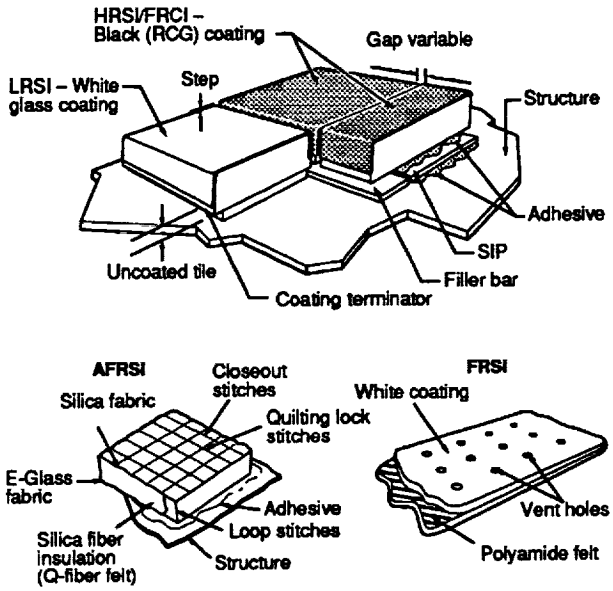

FIGURE 3: RSI SYSTEM CONFIGURATION

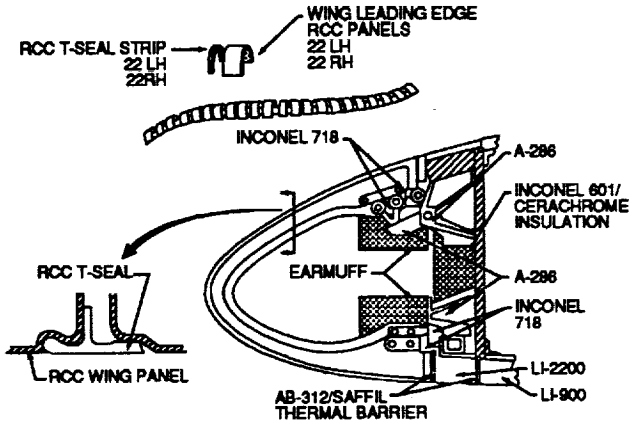

FIGURE 4: WING LEADING EDGE SYSTEM COMPONENTS

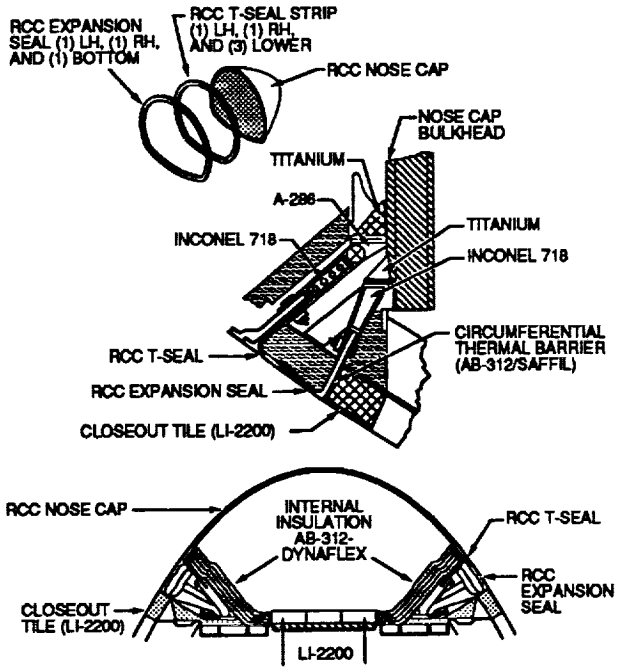

FIGURE 5: NOSE CAP SYSTEM COMPONENTS

The nylon felt is a strain isolation pad (SIP) used to isolate the low strength, brittle tile from airframe structural strains and deflections and subsequent critical tile stresses. Tiles are densified at the inner mold line to assure adequate strength at the tile/SIP interface. This densification was implemented to provide adequate tile structural margin for the predicted load cases. Tile-to-tile contact resulting from acoustic-induced tile movement or from contraction of the airframe in the cold extremes of space is prevented by providing gaps between the tiles. The filler bar material at the bottom of the tile-to-tile gap is used for thermal insulation from gap heating. In the higher pressure gradient regions of the Orbiter, open gaps could result in sufficient ingestion of high-temperature gas flow during entry, causing local overtemperature of the various TPS components and the structure. To preclude this from happening, two basic types of gap filler, "pillow" or "layer," are bonded to the top of filler bar. Thermal barriers made from the ceramic cloth, which are filled with soft insulation and/or metallic springs, are used to fill the larger gaps around movable hatches and doors. The RSI blankets are bonded directly to the structure with a silicone rubber adhesive.

The RCC wing leading edge (WLE), nose cap, and chin panel are structural fairings which transmit aerodynamic loads to the airframe structure through discrete mechanical attachments (figures 4, 5, 6). Inconel 718 and A-286 stainless steel fittings are bolted to flanges formed on the RCC components. They are attached to the aluminum wing spar and fuselage forward bulkhead. The fitting arrangement provides thermal isolation, allows for thermal expansion, and accommodates structural displacement. The WLE consists of 22 panels joined by 22 T-seals. This segmentation is necessary not only to facilitate the high-temperature fabrication process, but also to accommodate the thermal expansion during entry while preventing large gaps or interference between the parts. In addition, the T-seals prevent the ingestion of the hot boundary-layer gases into the wind leading edge cavity during entry. The nose cap and chin panel seal design and structural attachments are similar to the WLE. Since the RCC is not an insulator, the metallic attachments and adjacent aluminum structure must be protected from internal radiation and conduction by internal insulation blankets. This insulation consists of cerachrome insulation, contained in formed and welded Inconel foil, blankets fabricated from AB-312 ceramic cloth, saffil and cerachrome insulation, and ceramic tiles.

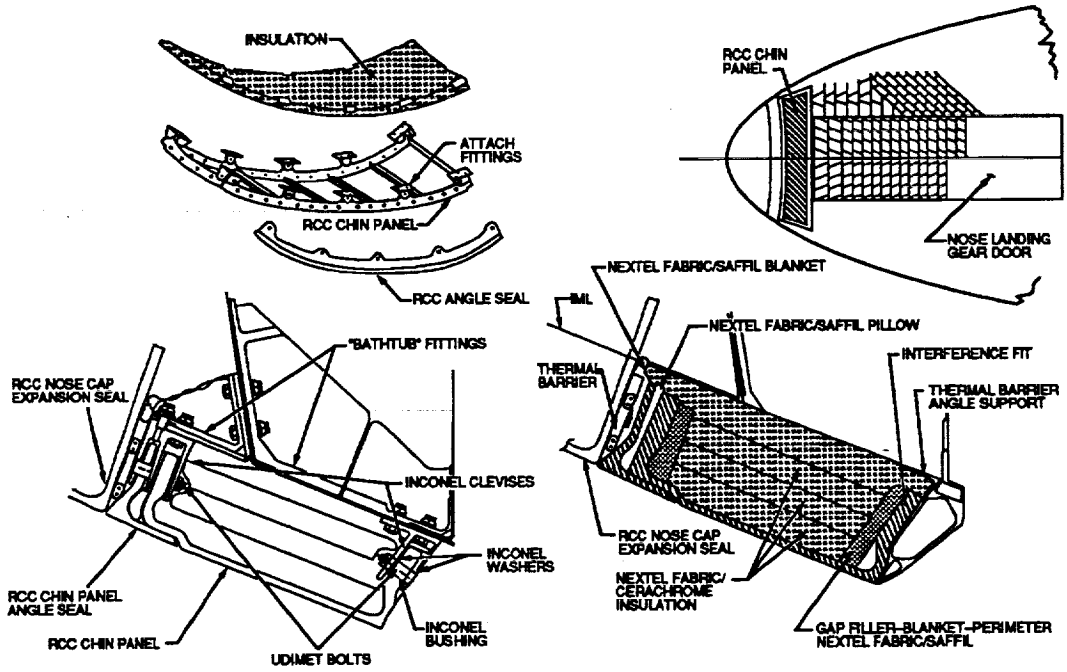

FIGURE 6: RCC CHIN PANEL SYSTEM COMPONENTS

FLIGHT EXPERIENCE

Aerothermodynamic Environment

The initial five Orbiter flights provided sufficient data to assess the aerothermal environment in terms of predicted and measured temperatures and surface heating rates. Detailed comparisons of selected flight data and vehicle locations with various theoretical aerothermodynamic heating techniques (i.e., chemical equilibrium, nonequilibrium flow, material finite catalycity, etc.) are available. These results indicate that nonequilibrium and surface catalysis effects, initially ignored in design, resulted in predicted heat fluxes greater than experienced in flight (figure 7). This provided an added margin of safety in the TPS design. Since these initial flights, operational flight data have been evaluated to identify any possible trends in Orbiter surface heating rates due to repeated exposure to both the natural and hypersonic reentry environments. Lower surface thermocouple results from 25 STS flights indicated that the heating rates were consistent from flight to flight. No clearly identifiable trends in the lower surface heating rates as a result of tile surface degradation (i.e., emissivity, catalysis) could be established.

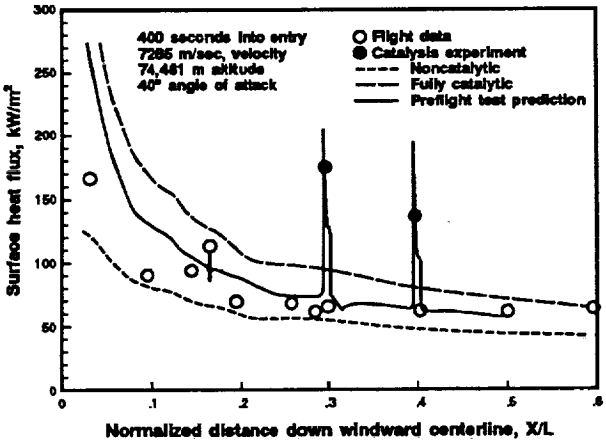

FIGURE 7: ORBITER INFERRED AND PREDICTED HEAT FLUX, STS-3

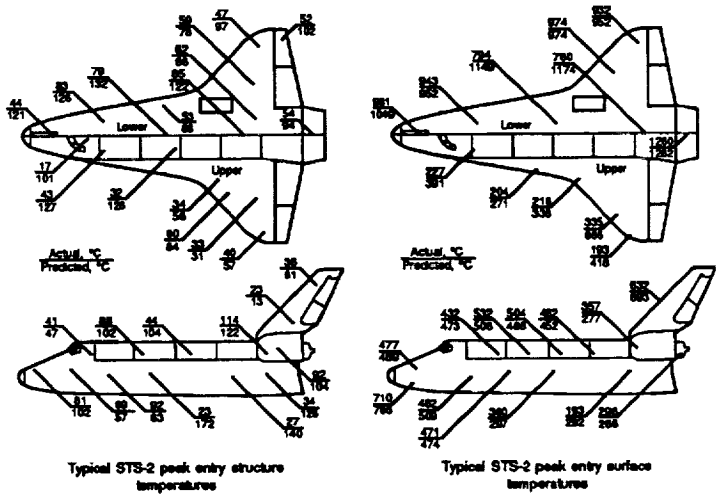

FIGURE 8: ORBITER ENTRY TEMPERATURES

TPS Thermal Performance

Thermal performance data were obtained during the STS-1 through STS-5 flight tests by means of the development flight instrumentation (DFI). The instrumentation consisted primarily of thermocouples located in RSI tile surfaces, at various depths in the RSI, at the structural bond line, and at numerous locations on the airframe structure. Noncontact radiometers were used to measure internal surface temperatures for selected RCC components. Figure 8 shows the distribution of actual predicted peak surface and structural temperatures experienced on the Orbiter Columbia during STS-2. In general, the predicted temperatures were higher than measured, which is attributed to noncatalytic surface heating effects and the exclusion of convective cooling effects in the thermal analysis models. The DFI flights provided sufficient engineering data, coupled with postflight inspections, to assess the thermostructural design and capability of the TPS components.

Radiometer measurement of WLE inner mold-line temperature (IML) as a function of semispan (figure 9) provided the data to establish WLE heating distribution (figure 10). The maximum heating zone at the 55-percent semispan results from the interaction of the nose cap bow shock and wing shock, which results in higher boundary layer pressures and heating rates. A comparison of measured temperatures of the RCC attachment hardware, internal insulation, and wing span structure are shown in figure 11. Predicted wing leading edge RCC surface temperatures for a nominal and high inclination, heavy weight entry are shown in figure 12. RCC is protected from oxidation by a silicon carbide coating which maintains a passive oxidation condition on the surface necessary for a multimission capability. A comparison of the active-passive transition oxygen pressures for SiC to nominal flight conditions (figure 13) indicates a passive state of oxidation during entry.

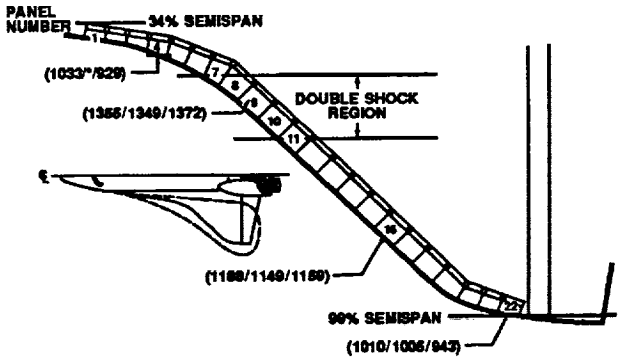

FIGURE 9: STS-2, STS-3, AND STS-5 PEAK IML TEMPERATURE (°C) LESS WING LEADING EDGE

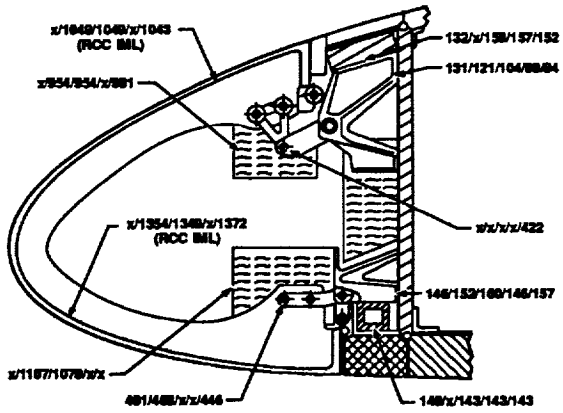

FIGURE 11: PANEL 9 PEAK TEMPERATURES, °C [X/X/X/X/X = STS-1/STS-2/STS-3/STS-4/STS-5, ORBITER VEHICLE 102]

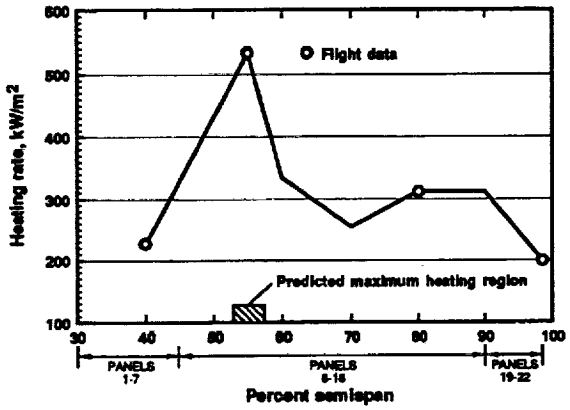

FIGURE 10: WING LEADING EDGE SPANWISE HEATING RATE

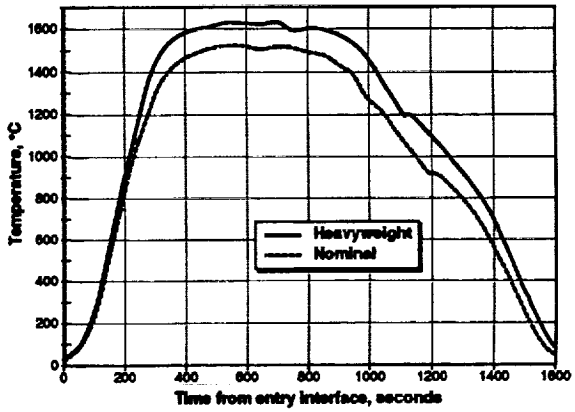

FIGURE 12: WING LEADING EDGE – PANEL 9 RCC SURFACE TEMPERATURES FOR HEAVYWEIGHT AND NOMINAL ENTRY

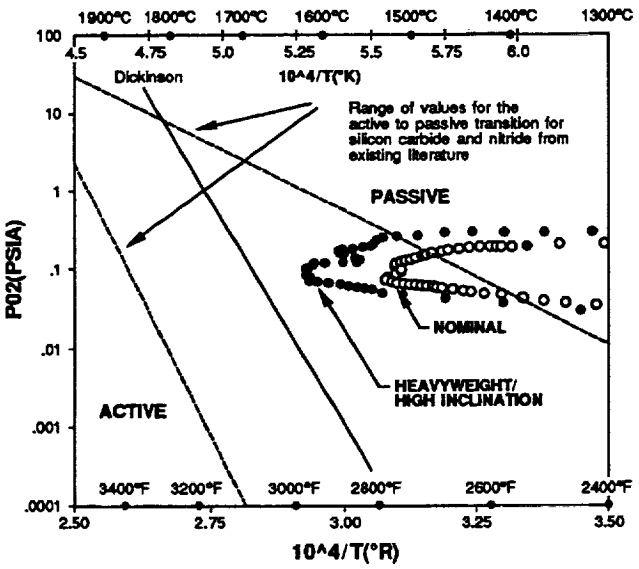

FIGURE 13: ACTIVE-PASSIVE TRANSITION OXYGEN PRESSURES COMPARISONS WITH FLIGHT CONDITIONS

Limited operational TPS data are obtained for every Orbiter flight (figures 14 and 15). These data are used to assess any changes in material performance with repeated reuse, flight-to-flight trajectory variations, and to assess flight anomalies. Through flight STS-57 no degradation in TPS performance has been observed. The TPS thermal performance database obtained from the DFI flights and subsequent operational flights has provided the data and confidence to extend the operational capability of the Orbiter.

TPS Thermal Mechanical Performance

The Shuttle Orbiter TPS flight experience based on postflight inspections can be summarized into the following areas: impact damage, gap filler damage and/or tile slumping, thermal barrier damage, and window contamination/impacts. The tiles have performed exceptionally well despite exposure to adverse weather conditions and debris damage during ascent. Since the RSI material has low resistance to impacts, minor surface damage in the form of dents, gouges, and coating chips has occurred during all flights. An Orbiter postflight debris damage summary is shown in figure 16, and damage locations on the lower surface for a specific flight are shown in figure 17. This damage results from the shuttle external tank (ET) insulation, insulation fragments from the Solid Rocket Booster (SRB), limited ice-frost from the ET/SRB's during launch, and debris at the landing site. The degree of RSI damage is directly related to the size and density of the debris (figures 18 and 19). The damage that has occurred has not resulted in any significant degradation of the overall Orbiter TPS thermal performance. Approximately 2-3 percent of the impacted tiles are replaced with the remainder of the impacted tiles being repaired through standard repair procedures. These repair procedures were developed prior to STS-1 and have been expanded based on flight experience. Improved insulation installation and inspection techniques for the ET and SRB have also helped to reduce the overall number of impacts. However, as shown in figure 16, impacts vary in size and quantity from flight to flight and do not appear to be something that can be eliminated.

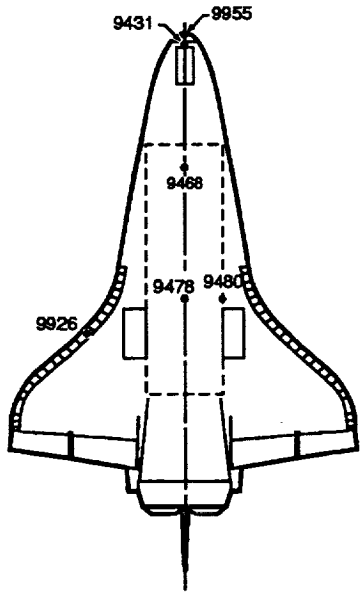

Flight	Vehicle	VO7T-9468	VO7T-9478	VO7T-9480	VO9T-9341	VO9T-9955	VO9T-9926
STS-1	OV-102	–	–	–	–	–	–
STS-2	OV-102	832	849	816	1138	–	1354**
STS-3	OV-102	1113*	799	743	–	–	1349**
STS-4	OV-102	–	–	–	–	–	–
STS-5	OV-102	954*	871*	760	1182	1429**	1372**
STS-26	OV-103	818	–	796	–	–	–
STS-27	OV-104	–	871	871	–	–	–
STS-29	OV-103	–	–	–	–	–	–
STS-30	OV-104	–	779	760	–	–	–
STS-28	OV-102	732	954	977	–	–	–
STS-34	OV-104	–	782	799	–	–	–
STS-33	OV-103	849	–	810	–	–	–
STS-32	OV-102	754	749	760	–	–	–
STS-36	OV-104	–	788	727	–	–	–
STS-31	OV-103	866	–	804	–	–	–
STS-41	OV-103	–	–	816	–	–	–
STS-38	OV-104	–	766	704	–	–	–
STS-35	OV-102	–	–	–	–	–	–
STS-37	OV-104	–	760	710	–	–	–
STS-39	OV-103	771	–	793	–	–	–
STS-40	OV-102	777	827	816	–	–	–
STS-43	OV-104	–	754	–	–	–	–
STS-48	OV-103	882	–	927	–	–	–
STS-44	OV-104	–	–	–	–	–	–

* Catalytic coated tile
** RCC inner surface

FIGURE 14: ORBITER PEAK SURFACE TEMPERATURES

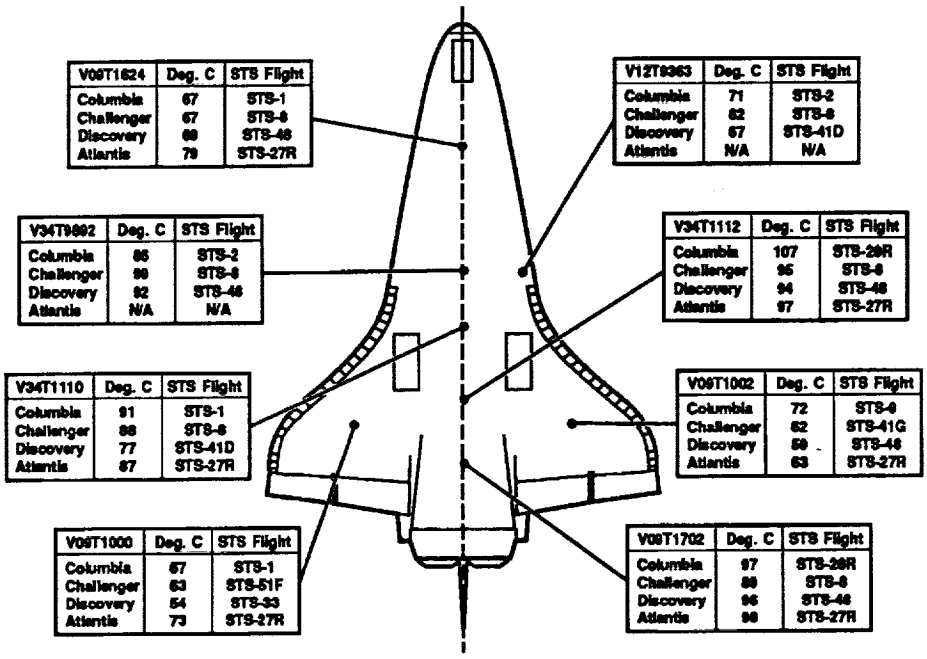

FIGURE 15: ORBITER MAXIMUM STRUCTURE TEMPERATURES

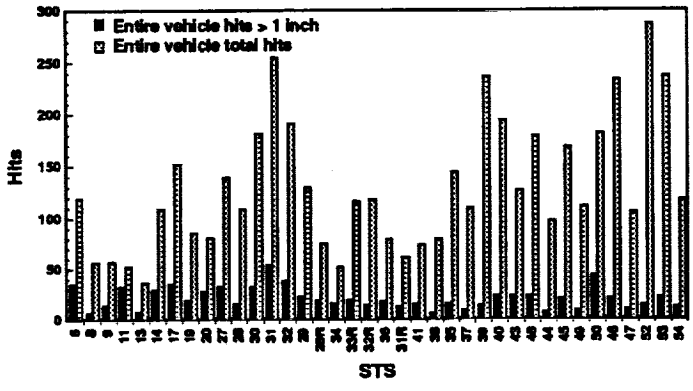

FIGURE 16: ORBITER DEBRIS DAMAGE SUMMARY FOR ENTIRE VEHICLE

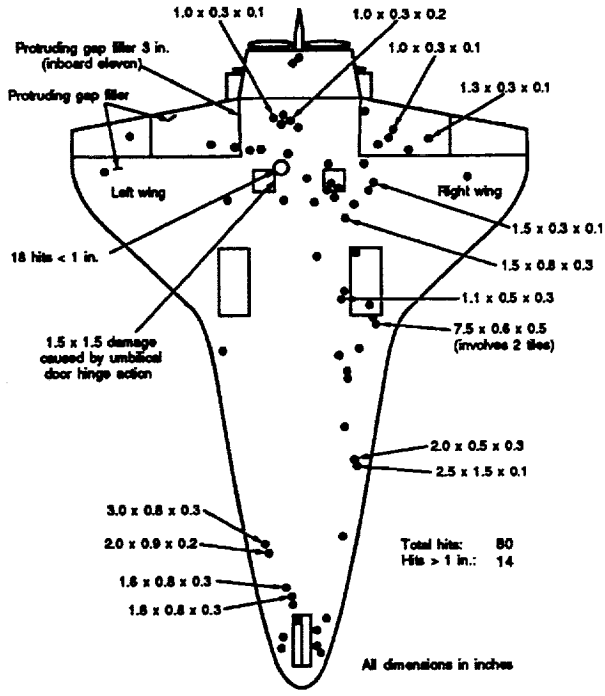

FIGURE 17: DEBRIS DAMAGE LOCATIONS

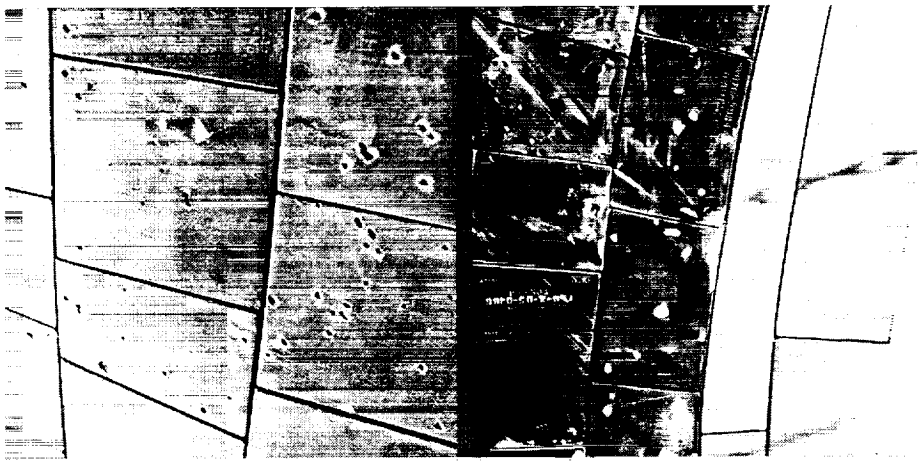

FIGURE 18: RSI TILE IMPACT DAMAGE

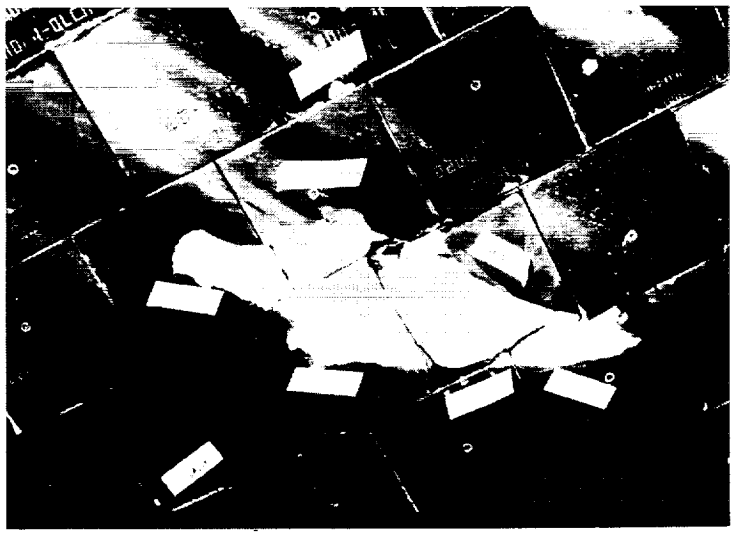

FIGURE 19: WING DEBRIS IMPACT GOUGE

Another TPS impact damage source is on-orbit debris and micrometeroids. Postflight inspection of the RSI tiles has not shown any damage from this source; however, impact damage to a RCC wing panel discovered during postflight inspection of STS-45 has been attributed to on-orbit debris. Two gouges in the leeward surface of the panel measuring 4.1 x 4.8 cm and 1.0 x 2.5 cm, respectively, were found (figure 20). Both impact areas resulted in coating spalling on the inner surface of the panel (figure 21), but no flow paths or through cracks were found. Chemical analyses determined that the object(s) that impacted the panel was of manmade origin and was not naturally occurring space debris. Oxidation of the carbon fibers in and around the craters was found. From the results of laboratory work, prelaunch data, and launch data, it has been determined that the damage occurred after the vehicle cleared the launch tower and before entry heating. Impact testing conducted at Rockwell and the Johnson Space Center indicates that the damage was caused by a manmade object traveling at low velocity.

Tile-to-tile gap heating has occurred in a number of locations and is usually observable from external inspection as slight tile shrinkage and/or slumping, filler bar charring, and gap filler degradation/breaching. An example of tile slumping and gap filler breaching is shown in figure 22. The use of higher density tiles and an improved gap filler design has significantly reduced the damage. An example of extensive damage as a result of gap heating, tile slumping, gap filler degradation, subsurface flow, and localized aluminum melting was found after STS-5 at the RCC nose cap/tile interface (figure 23). This area was subsequently redesigned with stiffer support structure and replacement of the tiles with an RCC panel, known as the chin panel.

Thermal barriers are utilized in the closeout areas between various components of the Orbiter and TPS, such as nose and main landing gear doors, rudder/speed brake, crew hatch, vent doors, payload bay doors, RCC/RSI interfaces, etc. Damage to these thermal barriers is unpredictable and caused by wear, flow paths (leaks), and impacts (figure 24). Damage has not been a

flight safety concern, but rather a turnaround or refurbishment issue (manpower). Design improvements to minimize postflight maintenance have been made by implementing mechanically attached barriers which improve fit and eliminate the time-intensive bonding process of the original design.

Another critical area on the Orbiter, not generally considered part of the TPS, is the window system. As shown in figure 25, the Orbiter has 11 windows (6 forward, 2 overhead, 1 side hatch and 2 rear view). The forward windows consist of three panes each: thermal, redundant, and pressure. Hazing or contamination (mainly from SRB separation) of the outer thermal pane occurs during each flight (figure 25). A cleaning procedure has been developed to remove the haze and maintain required visibility. The outer panels are also subject to impact, and very detailed inspections are performed after each flight to ensure structural integrity of the glass. Through flight STS-54, a total of 35 window panels have been replaced, 34 due to impact damage and 1 due to hazing.

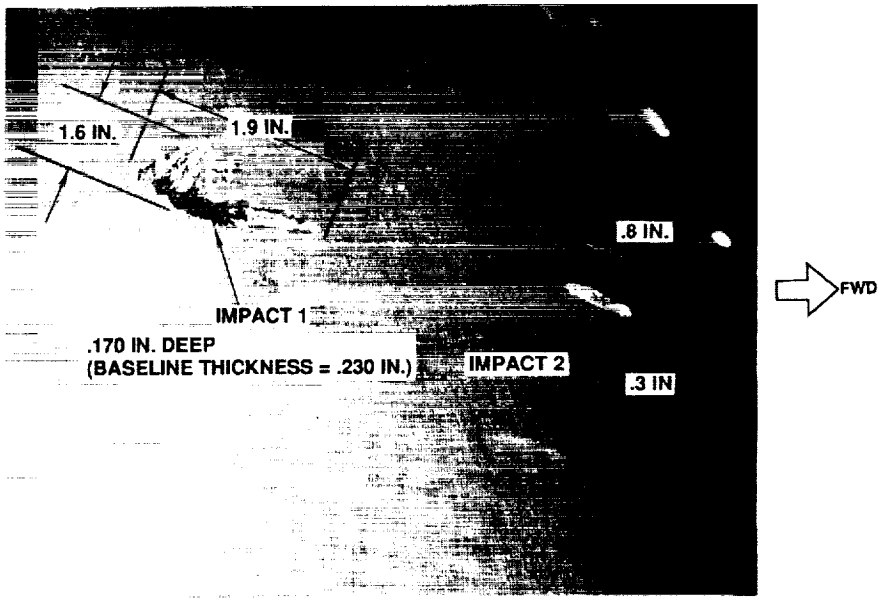

FIGURE 20: OV-104 WING LEADING EDGE, PANEL 10 RH OUTER MOLD LINE (OML)

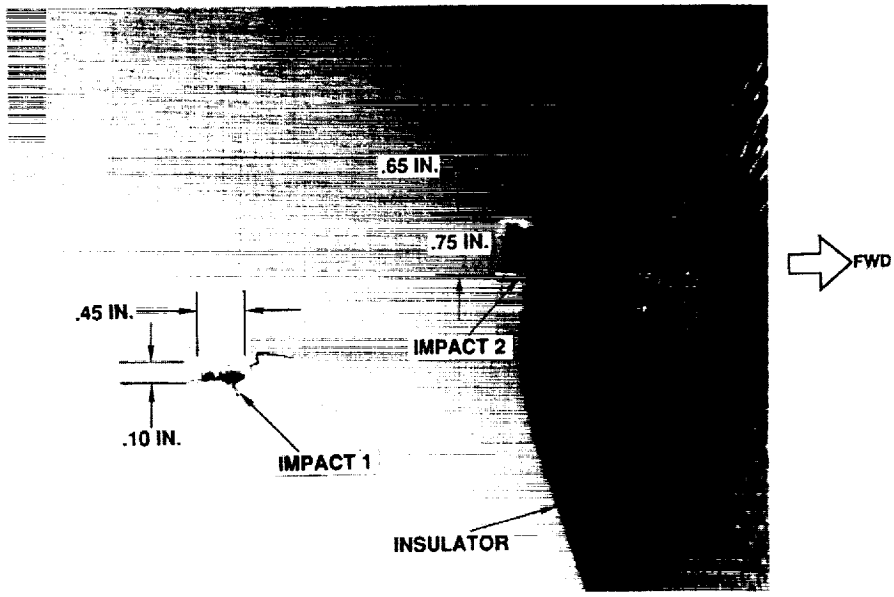

FIGURE 21: OV-104 WING LEADING EDGE, PANEL 10 RH INNER MOLD LINE (IML)

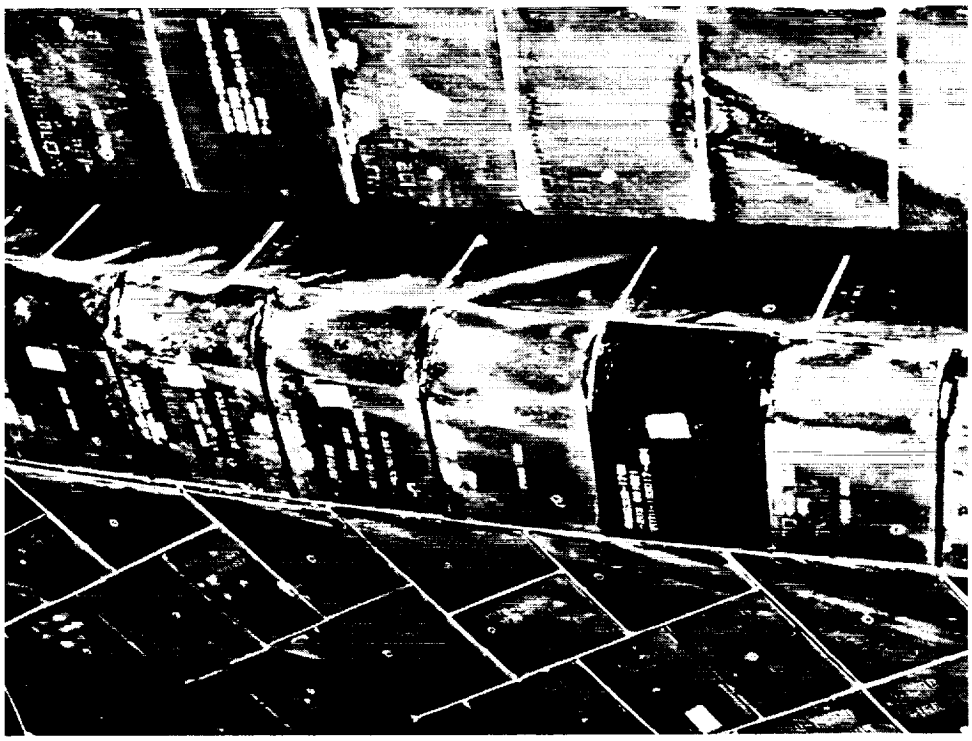

FIGURE 22: ELEVON–ELEVON GAP HEATING/TILE SLUMPING

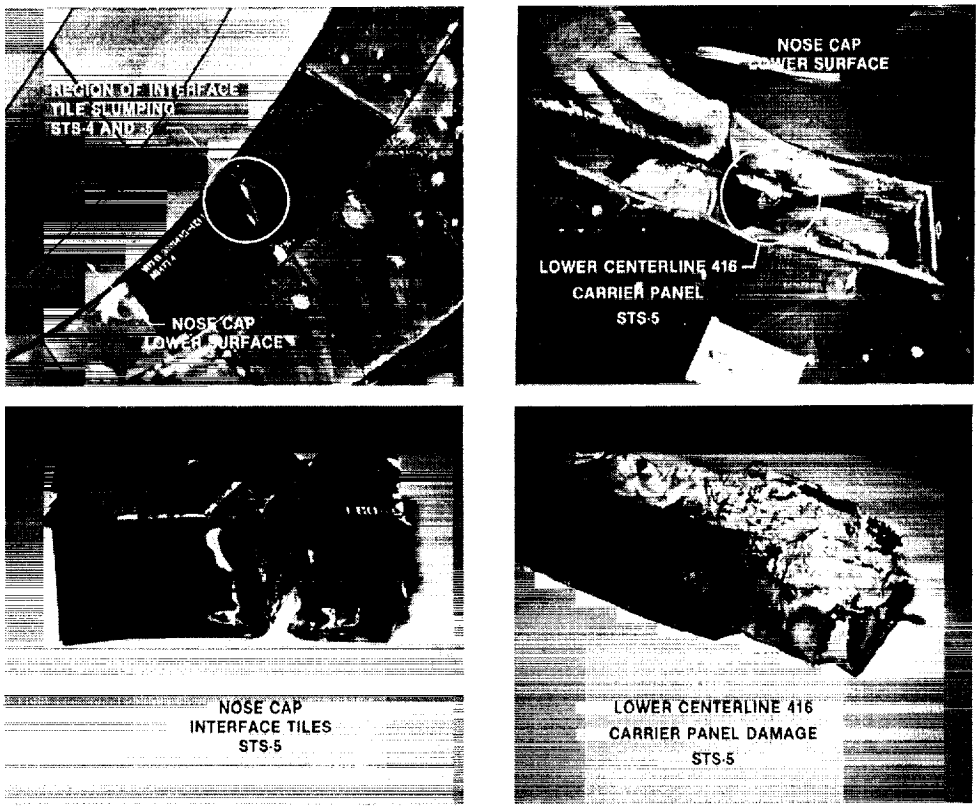

FIGURE 23: NOSE CAP LOWER SURFACE, INTERFACE DAMAGE, STS-5

FIGURE 24: NOSE LANDING GEAR DOOR THERMAL BARRIER

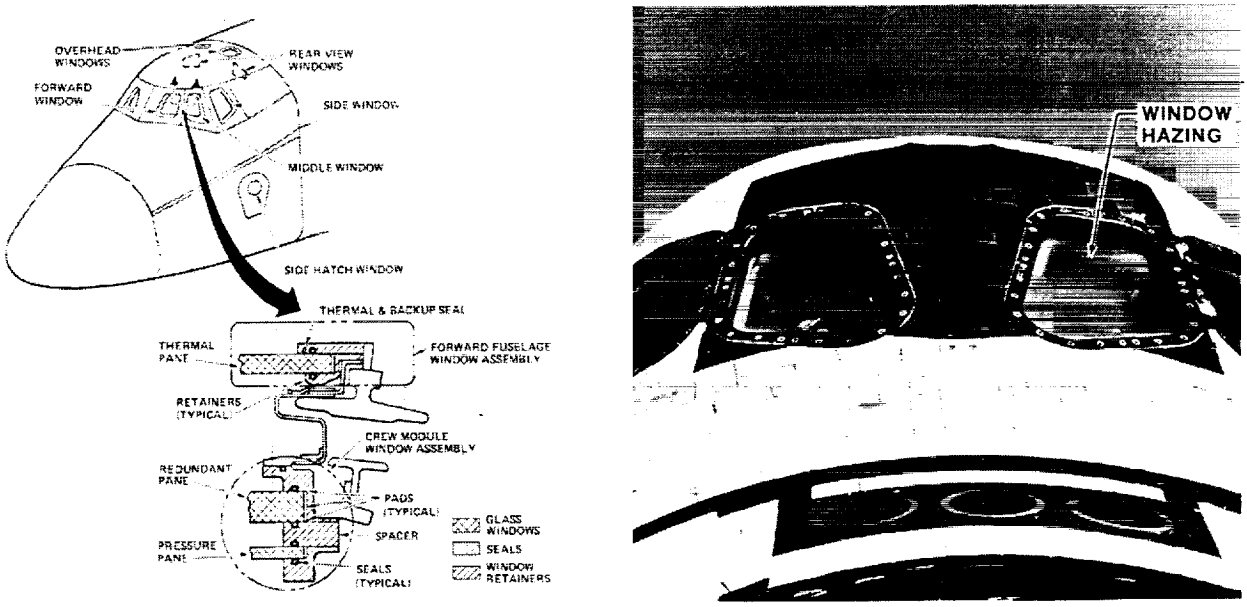

FIGURE 25: ORBITER WINDOW CONTAMINATION

Concluding Remarks

Fifty-five successful Orbiter flights have been accomplished since the first flight of Columbia on April 23, 1981. Outstanding thermal/structural performance during these flights indicates that the proper thermal protection materials and design approaches were selected for the Orbiter vehicles. There has been some localized damage, but these areas have been amenable to repair or minor design modifications. Degradation of the Orbiter TPS (RSI and RCC) has been minimal, and satisfactory vehicle operations have been established.

BIBLIOGRAPHY

Dotts, R. L.; Curry, D. M.; and Tillian, D. J.; "Orbiter Thermal Protection Systems," Space Shuttle Technical Conference, NASA CP-2342, Part 2, pp. 1061-1081, June 28-30, 1983.

Cunningham, J. A.; and Haney, J. W.; "Space Shuttle Wing Leading Edge Heating Environment Prediction Derived from Development Flight Data," Shuttle Performances: Lessons Learned; NASA CP-2283, Part 2, pp. 1083-1110, March 8-10, 1983.

Scott, C. D.; "Effects of Nonequilibrium and Wall Catalysis on Shuttle Heat Transfer," J. of Spacecraft and Rockets, Vol. 22, No. 5, Sept-Oct. 1985, pp. 489-499.

Lee, D. B.; and Harthun, M. H.; "Aerothermodynamic Entry Environment of the Space Shuttle Orbiter," AIAA paper no. 82-0821, June 1982.

Shappee, T. B.; and Bouslog, S. A.; "Evaluation of Heating Rate Trends on the Space Shuttle Orbiter," LESC-30208, April 1992.

Dotts, R. L.; Tillian, D. J.; and Smith, J. A.; "Space Shuttle Orbiter-Reusable Surface Insulation Flight Performance," Proceedings of AIAA/ASME/ASCE/AMS 23rd Structures, Structural Dynamics, and Materials Conference, pp. 16-22, New Orleans, LA, May 10-12, 1982.

Curry, D. M.; Johnson, D. W.; and Kelly, R. E.; "Space Shuttle Orbiter Leading Edge Flight Performance compared to Design Goals," Shuttle Performance: Lessons Learned, NASA CP-2283, Part 2, pp. 1065-1082, March 8-10, 1983.

Curry, D. M.; "Thermal Protection Systems – Manned Spacecraft Flight Experience," Current Technology for Thermal Protection Systems, NASA CP-3157, pp. 19-41, Feb. 1992

REPORT DOCUMENTATION PAGE

Form Approved
OMB No. 0704-0188

1. AGENCY USE ONLY *(Leave blank)*	2. REPORT DATE	3. REPORT TYPE AND DATES COVERED
	July 1993	final

4. TITLE AND SUBTITLE
SPACE SHUTTLE ORBITER THERMAL PROTECTION SYSTEM DESIGN AND FLIGHT EXPERIENCE

5. FUNDING NUMBERS

6. AUTHOR(S)

Donald M. Curry

7. PERFORMING ORGANIZATION NAME(S) AND ADDRESS(ES)

Lyndon B. Johnson Space Center
Houston, TX 77058

8. PERFORMING ORGANIZATION REPORT NUMBER

S-725

9. SPONSORING / MONITORING AGENCY NAME(S) AND ADDRESS(ES)

National Aeronautics and Space Administration
Washington, D.C. 20546

10. SPONSORING / MONITORING AGENCY REPORT NUMBER

TM-104773

11. SUPPLEMENTARY NOTES

Presented at the First ESA/ESTEC Workshop on Thermal Protection Systems
Noordwijk, the Netherlands, May 5-7, 1993

12a. DISTRIBUTION / AVAILABILITY STATEMENT

National Technical Information Service
5285 Port Royal Road
Springfield, VA 22161
(703) 487-4600

Subject Category: 34

12b. DISTRIBUTION CODE

13. ABSTRACT *(Maximum 200 words)*

The Space Shuttle Orbiter Thermal Protection System materials, design approaches associated with each material, and the operational performance experienced during fifty-five successful flights are described. The flights to date indicate that the thermal and structural design requirements have been met and that the overall performance has been outstanding.

14. SUBJECT TERMS
thermal protection systems, Shuttle Orbiter flight performance, orbital debris, aerothermodynamic environment

15. NUMBER OF PAGES
20

16. PRICE CODE

17. SECURITY CLASSIFICATION OF REPORT	18. SECURITY CLASSIFICATION OF THIS PAGE	19. SECURITY CLASSIFICATION OF ABSTRACT	20. LIMITATION OF ABSTRACT
Unclassified	Unclassified	Unclassified	Unlimited